Geophys. J. Int. (2006) **166,** 418–434 doi: 10.1111/j.1365-246X.2006.02921.x

Quasi-static internal deformation due to a dislocation source in a multilayered elastic/viscoelastic half-space and an equivalence theorem

Yukitoshi Fukahata and Mitsuhiro Matsu'ura

Department of Earth and Planetary Science, University of Tokyo, Tokyo 113-0033*, Japan. E-mail: fukahata@eps.s.u-tokyo.ac.jp*

Accepted 2006 January 17. Received 2006 January 17; in original form 2005 September 5

SUMMARY

We have obtained general expressions for quasi-static internal deformation fields due to a dislocation source in a multilayered elastic/viscoelastic half-space under gravity by applying the correspondence principle of linear viscoelasticity to the associated elastic solution (Fukahata & Matsu'ura 2005). The use of the upgoing propagator matrix for the region below the source and the downgoing propagator matrix for the region above the source in the derivation of mathematical expressions guarantees the numerical stability of the obtained viscoelastic solution over the whole region. The viscoelastic deformation fields due to a dislocation source tend to a certain steady state with the progress of viscoelastic stress relaxation. The completely relaxed viscoelastic solution can be directly obtained from the associated elastic solution by taking the rigidity of the elastic layer corresponding to a Maxwell viscoelastic layer to be zero. We gave an explicit mathematical proof of this theoretical relationship, which we named the equivalence theorem, on the basis of the correspondence principle of linear viscoelasticity and the limiting value theorem of the Laplace transform. The equivalence theorem is applicable not only to the elastic-viscoelastic stratified medium but also to general elastic and linear-viscoelastic composite media. As numerical examples we show the quasi-static internal displacement fields due to strike-slip motion on a vertical fault and dip-slip motion on a subduction plate boundary in an elastic surface layer overlying a viscoelastic half-space. The temporal variation of the computed deformation fields shows that the effective relaxation time of the elastic-viscoelastic system is much longer than the Maxwell relaxation time defined by the ratio of viscosity to rigidity in the viscoelastic layer.

Key words: crustal deformation, dislocation theory, equivalence theorem, layered medium, viscoelasticity.

1 INTRODUCTION

In the computation of crustal deformation elastic half-space models have been widely used for simplicity. The elastic half-space may be a reasonable assumption as far as short-term crustal deformation, such as coseismic deformation, is concerned. To long-term crustal deformation such as interseismic deformation and post-glacial rebound, however, the elastic half-space model is no longer applicable, because the effects of viscoelastic stress relaxation in the asthenosphere underlying the elastic lithosphere cannot be neglected (Thatcher & Rundle 1984; Matsu'ura & Sato 1989; Fukahata *et al.* 2004).

Viscoelastic responses due to a dislocation source in an elastic-viscoelastic layered half-space have already been obtained by Rundle (1978, 1982), Matsu'ura *et al.* (1981) and Iwasaki & Matsu'ura (1981) for surface displacements and strains. Their formulations have been applied to post-seismic crustal deformation due to viscoelastic stress relaxation in the asthenosphere (Matsu'ura & Iwasaki 1983), crustal deformation associated with earthquake cycles (Thatcher & Rundle 1984; Matsu'ura & Sato 1989; Fukahata *et al.* 2004), and long-term crustal deformation due to mechanical interaction at convergent plate boundaries (Sato & Matsu'ura 1993; Takada & Matsu'ura 2004; Hashimoto *et al.* 2004). In modelling earthquake generation cycles, however, we need to evaluate internal deformation fields due to fault slip, because the physical process of earthquake generation cycles is governed by a coupled non-linear system, consisting of a slip-response function that relates fault slip to shear stress change, a fault constitutive relation that prescribes change in shear strength with fault slip or slip velocity, and relative plate motion as a driving force (Tse & Rice 1986; Stuart 1988; Hashimoto & Matsu'ura 2000, 2002; Matsu'ura 2005). Computation

of internal deformation fields due to fault slip is also needed in estimating pressure–temperature–time paths and modelling thermal structure evolution at plate convergence zones (England & Thompson 1984; Barr & Dahlen 1989; Fukahata & Matsu'ura 2000).

Extending the formulation of Matsu'ura *et al.* (1981), Matsu'ura & Sato (1997) have obtained expressions for internal deformation fields due to strike-slip motion on a vertical fault in an elastic layer overlying a viscoelastic half-space. Their expressions are, however, numerically unstable below the source depth, because they used only the downgoing propagator matrix in the derivation of the internal deformation fields (Fukahata & Matsu'ura 2005). Using both the upgoing and the downgoing propagator matrices and extending the formulation of Pan (1989), Pan (1997) derived a numerically stable solution of internal deformation for a layered transversely isotropic elastic medium. Recently, introducing the generalized propagator matrix, Fukahata & Matsu'ura (2005) have illuminated the relationship between the upgoing algorithm proposed by Singh (1970) and the downgoing algorithm proposed by Sato (1971), and obtained the complete expressions for internal deformation fields due to a dislocation source in a multilayered elastic half-space. That is, they have completely solved the numerical instability problem at large wavenumber (e.g. Singh 1970; Jovanovich *et al.* 1974; Rundle 1978, 1982; Ma & Kusznir 1992; Matsu'ura & Sato 1997). In general, the viscoelastic solution can be obtained from the associated elastic solution by applying the correspondence principle of linear viscoelasticity (Lee 1955; Radok 1957). In the present study, we apply the correspondence principle to the elastic solution derived by Fukahata & Matsu'ura (2005), and obtain general expressions for quasi-static internal deformation fields due to a dislocation source in a multilayered elastic/viscoelastic half-space under gravity.

The quasi-static deformation fields due to a dislocation source tend to a certain steady state with the progress of viscoelastic stress relaxation. In some problems we are not interested in the process of stress relaxation, but in the steady state after complete relaxation. From consideration of the constitutive equations, Cohen (1980a,b) has derived effective reduced elastic moduli at completely relaxed states. By using the effective reduced moduli he obtained the surface deformation fields due to a strike slip after the completion of stress relaxation directly from the associated elastic solution. Following Cohen's idea, Ma & Kusznir (1994a,b) computed internal deformation fields after the complete relaxation of the viscoelastic substratum by taking the rigidity of elastic substratum to be very small in the associated elastic solution. For vertical surface displacements due to a pure dip-slip, Ma & Kusznir (1995) have numerically confirmed that the deformation fields obtained from the associated elastic solution by this approach almost coincides with those calculated from the viscoelastic solution by taking the time t to be infinity. In the present paper we prove the mathematical equivalence between the completely relaxed viscoelastic solution and the associated elastic solution with the corresponding elastic layer having zero rigidity, on the basis of the correspondence principle of linear viscoelasticity and the limiting value theorem of the Laplace transform.

2 MATHEMATICAL FORMULATION

We consider n-1 parallel layers overlying a half-space. Every layer and interface is numbered in ascending order from the free surface as shown in Fig. 1(a). The jth layer is bounded by the (j-1)th and jth interfaces. The depth of the jth interface is denoted by H_j, and the thickness of the jth layer by $h_j = H_j - H_{j-1}$. Each parallel layer is homogeneous, isotropic, and elastic or viscoelastic. The rheological property of the viscoelastic layers is assumed to be Maxwell in shear and elastic in bulk. Then, we may write the constitutive equations for elastic layers as

$$\sigma_{ij} = \lambda_l \varepsilon_{kk} \delta_{ij} + 2\mu_l \varepsilon_{ij}, \tag{1}$$

and for viscoelastic layers as

$$\dot{\sigma}_{ij} + \frac{\mu_l}{\eta_l}\left(\sigma_{ij} - \frac{1}{3}\sigma_{kk}\delta_{ij}\right) = \lambda_l \dot{\varepsilon}_{kk}\delta_{ij} + 2\mu_l \dot{\varepsilon}_{ij}, \tag{2}$$

where σ_{ij} and ε_{ij} are the stress and strain tensors, respectively, λ_l and μ_l denote the Lamé elastic constants in the lth layer, η_l is the viscosity in the lth layer, and the dot means differentiation with respect to time. Here, it should be noted that the Laplace transform of eq. (2) yields

$$\tilde{\sigma}_{ij} = \hat{\lambda}_l(s)\tilde{\varepsilon}_{kk}\delta_{ij} + 2\hat{\mu}_l(s)\tilde{\varepsilon}_{ij}, \tag{3}$$

with

$$\hat{\lambda}_l(s) = \frac{\lambda_l \tau_l s + K_l}{\tau_l s + 1}, \quad \hat{\mu}_l(s) = \frac{\tau_l s \mu_l}{\tau_l s + 1}, \tag{4}$$

and

$$\tau_l = \frac{\eta_l}{\mu_l}, \tag{5}$$

where K_l is the bulk modulus in the lth layer, s is the Laplace transform variable, and the tilde denotes the Laplace transform of the corresponding physical quantity. From comparison of eqs (1) and (3), we can see that the Laplace transform of the constitutive equation for the viscoelastic medium is formally identical with that for the elastic medium, except that the Lamé constants are replaced by the s-dependent moduli $\hat{\lambda}_l(s)$ and $\hat{\mu}_l(s)$.

First, we consider an elastic problem associated with the viscoelastic problem, where each viscoelastic layer is replaced by a perfectly elastic layer with the corresponding elastic constants. According to the correspondence principle of linear viscoelasticity (Lee 1955; Radok 1957), the Laplace transform of the viscoelastic solution is directly obtained from the associated elastic solution by replacing the source time function with its Laplace transform and the elastic constants, λ_l and μ_l, of the layers corresponding to the viscoelastic layers with the s-dependent moduli, $\hat{\lambda}_l(s)$ and $\hat{\mu}_l(s)$, respectively. Operation of the inverse Laplace transform on the s-dependent solution yields the viscoelastic solution in the time domain.

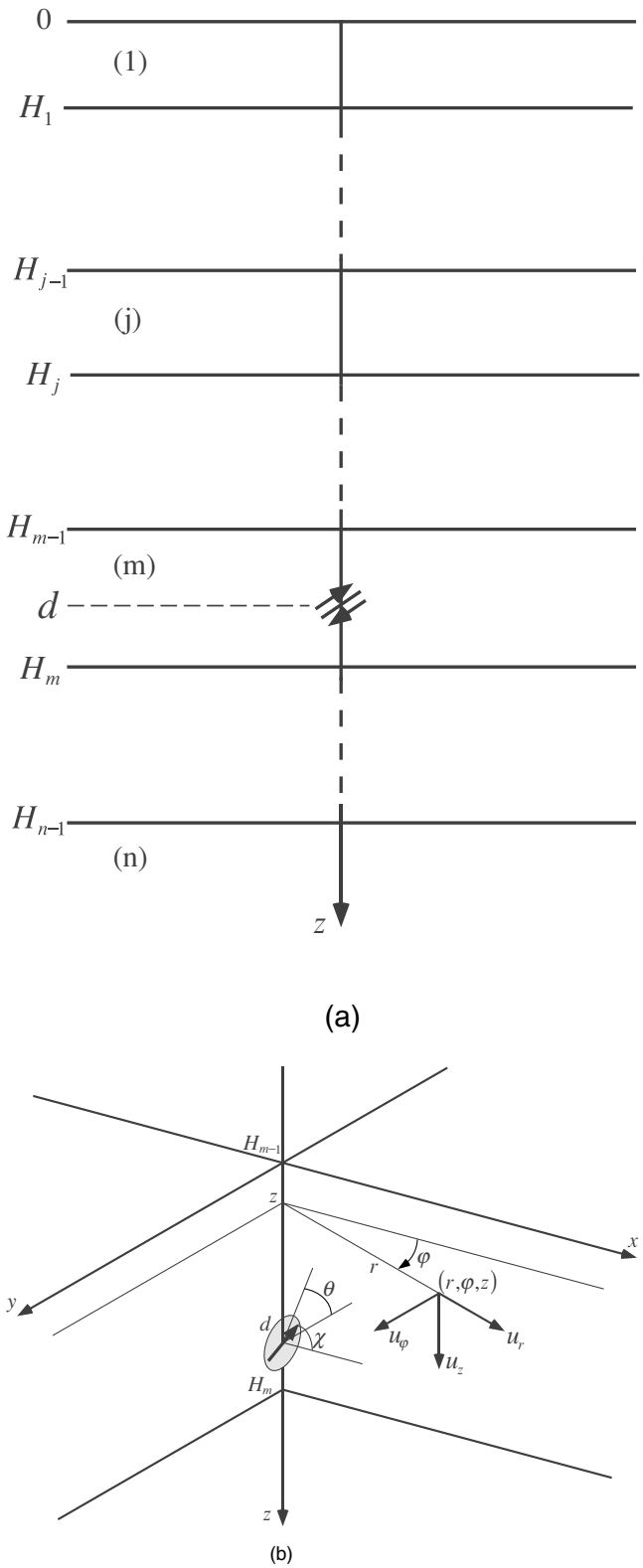

Figure 1. The coordinate system, fault geometry, and notations. (a) Numbering of the layers and interfaces. The jth layer is bounded by the (j-1)th and jth interfaces. The depth of the jth interface is denoted by H_j, and the thickness of the jth layer by $h_j(= H_j - H_{j-1})$. A point dislocation source is located in the mth layer. Each layer is elastic or viscoelastic. (b) Cylindrical (r, φ, z) and Cartesian (x, y, z) coordinate systems used. The point dislocation source with a dip angle θ and a slip angle χ is located at depth d on the z-axis.

2.1 The associated elastic solutions

We consider the associated elastic problem in which each viscoelastic layer is replaced by a perfectly elastic layer with the corresponding elastic constants. Then, the complete solution of the associated elastic problem is given in Fukahata & Matsu'ura (2005). In their expressions for the internal elastic deformation fields, the elastic constants μ_l and γ_l are used instead of λ_l and μ_l, where γ_l is defined by

$$\gamma_l = \frac{\lambda_l + \mu_l}{\lambda_l + 2\mu_l}. \tag{6}$$

In the following part of this section we explicitly describe the dependence of the physical quantities on the elastic constants, μ_l and γ_l, for convenience of the derivation of the viscoelastic solution.

We take a cylindrical coordinate system (r, φ, z) as shown in Fig. 1(b). The positive z-axis is taken as directed into the medium. A tangential displacement discontinuity (dislocation) $\Delta u H(t)$ occurs over a unit infinitesimal area at $(0, 0, d)$ in the mth layer $(1 \le m \le n)$ with a dip angle θ and a slip angle χ. Here, $H(t)$ denotes a unit step function. Then, the elastic displacement components u_i^E $(i = r, \varphi, z)$ and stress components σ_{zi}^E $(i = r, \varphi, z)$ in the jth layer due to the dislocation source are given by the following semi-infinite integrals with respect to wavenumber ξ:

$$\begin{cases} u_r^E(r,\varphi,z,t;j;\mu_l,\gamma_l) = H(t)\dfrac{\Delta u}{4\pi}\left[\displaystyle\int_0^\infty \mathbf{Y}_1^E(z;\xi;j;\mu_l,\gamma_l)\partial_r\mathbf{J}(r,\varphi;\xi)\,d\xi + \int_0^\infty \mathbf{Y}_1'^E(z;\xi;j;\mu_l)\frac{1}{r}\partial_\varphi\mathbf{J}'(r,\varphi;\xi)\,d\xi\right] \\ u_\varphi^E(r,\varphi,z,t;j;\mu_l,\gamma_l) = H(t)\dfrac{\Delta u}{4\pi}\left[\displaystyle\int_0^\infty \mathbf{Y}_1^E(z;\xi;j;\mu_l,\gamma_l)\frac{1}{r}\partial_\varphi\mathbf{J}(r,\varphi;\xi)\,d\xi - \int_0^\infty \mathbf{Y}_1'^E(z;\xi;j;\mu_l)\partial_r\mathbf{J}'(r,\varphi;\xi)\,d\xi\right] \\ u_z^E(r,\varphi,z,t;j;\mu_l,\gamma_l) = H(t)\dfrac{\Delta u}{4\pi}\displaystyle\int_0^\infty \xi\mathbf{Y}_2^E(z;\xi;j;\mu_l,\gamma_l)\mathbf{J}(r,\varphi;\xi)\,d\xi \end{cases} \tag{7}$$

and

$$\begin{cases} \sigma_{zr}^E(r,\varphi,z,t;j;\mu_l,\gamma_l) = H(t)\dfrac{\Delta u\mu_j}{4\pi}\left[\displaystyle\int_0^\infty 2\xi\mathbf{Y}_3^E(z;\xi;j;\mu_l,\gamma_l)\partial_r\mathbf{J}(r,\varphi;\xi)\,d\xi + \int_0^\infty \xi\mathbf{Y}_2'^E(z;\xi;j;\mu_l)\frac{1}{r}\partial_\varphi\mathbf{J}'(r,\varphi;\xi)\,d\xi\right] \\ \sigma_{z\varphi}^E(r,\varphi,z,t;j;\mu_l,\gamma_l) = H(t)\dfrac{\Delta u\mu_j}{4\pi}\left[\displaystyle\int_0^\infty 2\xi\mathbf{Y}_3^E(z;\xi;j;\mu_l,\gamma_l)\frac{1}{r}\partial_\varphi\mathbf{J}(r,\varphi;\xi)\,d\xi - \int_0^\infty \xi\mathbf{Y}_2'^E(z;\xi;j;\mu_l)\partial_r\mathbf{J}'(r,\varphi;\xi)\,d\xi\right] \\ \sigma_{zz}^E(r,\varphi,z,t;j;\mu_l,\gamma_l) = H(t)\dfrac{\Delta u\mu_j}{4\pi}\displaystyle\int_0^\infty 2\xi^2\mathbf{Y}_4^E(z;\xi;j;\mu_l,\gamma_l)\mathbf{J}(r,\varphi;\xi)\,d\xi, \end{cases} \tag{8}$$

where the superscript E denotes quantities related to the associated elastic solution. The z-independent vectors $\mathbf{J}$ and $\mathbf{J}'$ are defined by

$$\mathbf{J}(r,\varphi;\xi) = \begin{pmatrix} a_0(\varphi)J_0(\xi r) \\ a_1(\varphi)J_1(\xi r) \\ a_2(\varphi)J_2(\xi r) \end{pmatrix}, \quad \mathbf{J}'(r,\varphi;\xi) = \partial_\varphi \begin{pmatrix} a_1(\varphi)J_1(\xi r) \\ a_2(\varphi)J_2(\xi r) \end{pmatrix}, \tag{9}$$

with

$$\begin{cases} a_0(\varphi) = \frac{1}{4}\sin\chi\sin 2\theta \\ a_1(\varphi) = -\sin\chi\cos 2\theta\sin\varphi + \cos\chi\cos\theta\cos\varphi \\ a_2(\varphi) = \frac{1}{4}\sin\chi\sin 2\theta\cos 2\varphi + \frac{1}{2}\cos\chi\sin\theta\sin 2\varphi \end{cases} \tag{10}$$

Here, $J_k(\xi r)$ denotes the Bessel function of order k. The z-dependent kernel vectors $\mathbf{Y}_k^E$ $(k = 1, 2, 3, 4)$ and $\mathbf{Y}_k'^E$ $(k = 1, 2)$ compose the 4×3 and 2×2 deformation matrices $\mathbf{Y}^E$ and $\mathbf{Y}'^E$, respectively, as

$$\mathbf{Y}^E(z;j;\mu_l,\gamma_l) = \begin{pmatrix} \mathbf{Y}_1^E(z;j;\mu_l,\gamma_l) \\ \mathbf{Y}_2^E(z;j;\mu_l,\gamma_l) \\ \mathbf{Y}_3^E(z;j;\mu_l,\gamma_l) \\ \mathbf{Y}_4^E(z;j;\mu_l,\gamma_l) \end{pmatrix}, \quad \mathbf{Y}'^E(z;j;\mu_l) = \begin{pmatrix} \mathbf{Y}_1'^E(z;j;\mu_l) \\ \mathbf{Y}_2'^E(z;j;\mu_l) \end{pmatrix}. \tag{11}$$

Hereafter we omit the ξ-dependence for simplicity. In obtaining the deformation matrices, as demonstrated by Fukahata & Matsu'ura (2005), we must use the downgoing algorithm for $z < d$ and the upgoing algorithm for $z > d$ to suppress numerical instability. Then, we can express the deformation matrices in the following form:

$$\begin{cases} \mathbf{Y}^E(z;j;\mu_l,\gamma_l) = \exp(-q\xi)\mathbf{S}_{jm}(z;\mu_l,\gamma_l) + \delta_{nj}\delta_{\mathrm{nm}}\exp(-|z-d|\,\xi)\mathbf{Y}^s(z;\gamma_n) \\ \mathbf{Y}'^E(z;j;\mu_l) = \exp(-q\xi)\mathbf{S}'_{jm}(z;\mu_l) + \delta_{nj}\delta_{\mathrm{nm}}\exp(-|z-d|\,\xi)\mathbf{Y}'^s(z) \end{cases}, \tag{12}$$

with

$$q = \begin{cases} |z-d| & (j \ne n \text{ or } m \ne n) \\ z + d - 2H_{n-1} & (j = m = n) \end{cases}, \tag{13}$$

where δ_{nj} and δ_{nm} represent the Kronecker delta. The explicit expressions for $\mathbf{S}_{jm}^{(\prime)}$ and $\mathbf{Y}^{(\prime)s}$ are given in the Appendix. Here, $\mathbf{S}_{jm}^{(\prime)}$ represents $\mathbf{S}_{jm}$ or $\mathbf{S}'_{jm}$, and $\mathbf{Y}^{(\prime)s}$ represents $\mathbf{Y}^s$ or $\mathbf{Y}'^s$.

2.2 Viscoelastic solution

According to the correspondence principle, we can directly obtain the Laplace transform of the viscoelastic displacement components $\tilde{u}_i \quad (i = r, \varphi, z)$ and stress components $\tilde{\sigma}_{zi}(i = r, \varphi, z)$ by replacing $H(t)$ with $1/s$ and μ_l and γ_l corresponding to the viscoelastic layers with $\hat{\mu}_l(s)$ and $\hat{\gamma}_l(s)$ in eqs (7) and (8):

$$\begin{cases} \tilde{u}_r(r,\varphi,z,s;j) = \dfrac{\Delta u}{4\pi}\left[\displaystyle\int_0^\infty \tilde{\mathbf{Y}}_1(z,s;j)\partial_r \mathbf{J}(r,\varphi)\,d\xi + \int_0^\infty \tilde{\mathbf{Y}}'_1(z,s;j)\frac{1}{r}\partial_\varphi \mathbf{J}'(r,\varphi)\,d\xi\right] \\ \tilde{u}_\varphi(r,\varphi,z,s;j) = \dfrac{\Delta u}{4\pi}\left[\displaystyle\int_0^\infty \tilde{\mathbf{Y}}_1(z,s;j)\frac{1}{r}\partial_\varphi \mathbf{J}(r,\varphi)\,d\xi - \int_0^\infty \tilde{\mathbf{Y}}'_1(z,s;j)\partial_r \mathbf{J}'(r,\varphi)\,d\xi\right] \\ \tilde{u}_z(r,\varphi,z,s;j) = \dfrac{\Delta u}{4\pi}\displaystyle\int_0^\infty \xi\,\tilde{\mathbf{Y}}_2(z,s;j)\mathbf{J}(r,\varphi)\,d\xi, \end{cases} \tag{14}$$

$$\begin{cases} \tilde{\sigma}_{zr}(r,\varphi,z,s;j) = \dfrac{\Delta u\mu_j}{4\pi}\left[\displaystyle\int_0^\infty 2\xi\,\tilde{\mathbf{Y}}_3(z,s;j)\partial_r \mathbf{J}(r,\varphi)\,d\xi + \int_0^\infty \xi\,\tilde{\mathbf{Y}}'_2(z,s;j)\frac{1}{r}\partial_\varphi \mathbf{J}'(r,\varphi)\,d\xi\right] \\ \tilde{\sigma}_{z\varphi}(r,\varphi,z,s;j) = \dfrac{\Delta u\mu_j}{4\pi}\left[\displaystyle\int_0^\infty 2\xi\,\tilde{\mathbf{Y}}_3(z,s;j)\frac{1}{r}\partial_\varphi \mathbf{J}(r,\varphi)\,d\xi - \int_0^\infty \xi\,\tilde{\mathbf{Y}}'_2(z,s;j)\partial_r \mathbf{J}'(r,\varphi)\,d\xi\right] \\ \tilde{\sigma}_{zz}(r,\varphi,z,s;j) = \dfrac{\Delta u\mu_j}{4\pi}\displaystyle\int_0^\infty 2\xi^2\,\tilde{\mathbf{Y}}_4(z,s;j)\mathbf{J}(r,\varphi)\,d\xi, \end{cases} \tag{15}$$

where

$$\begin{cases} \tilde{\mathbf{Y}}_k(z,s;j) = \dfrac{1}{s}\mathbf{Y}^E_k(z;j;\hat{\mu}_l,\hat{\gamma}_l) & (k=1,2,3,4) \\ \tilde{\mathbf{Y}}'_k(z,s;j) = \dfrac{1}{s}\mathbf{Y}'^E_k(z;j;\hat{\mu}_l) & (k=1,2), \end{cases} \tag{16}$$

with

$$\hat{\gamma}_l(s) = \frac{\gamma_l s + \kappa_l}{s + \kappa_l}, \tag{17}$$

and

$$\kappa_l = \frac{4\gamma_l - 1}{3\tau_l}. \tag{18}$$

Here, we assumed the jth layer to be elastic. As shown in the next subsection, $\mathbf{Y}^E_k(z;j;\hat{\mu}_l,\hat{\gamma}_l)$ and $\mathbf{Y}'^E_k(z;j;\hat{\mu}_l)$ in eq. (16) can be expressed as the rational functions of the Laplace transform variable s in the following form:

$$\mathbf{Y}^{(\prime)E}_k(z;j;\hat{\mu}_l,\hat{\gamma}_l) = \frac{\sum_{i=0}^M \mathbf{a}^{(i)}s^i}{\sum_{i=0}^M b^{(i)}s^i}, \tag{19}$$

with

$$\frac{\mathbf{a}^{(M)}}{b^{(M)}} = \mathbf{Y}^{(\prime)E}_k(z;j;\mu_l,\gamma_l). \tag{20}$$

Here, it should be noted that $\mathbf{Y}'^E_k$ does not depend on $\hat{\gamma}_l$ in reality, and so the degree M of the polynomials for $\mathbf{Y}'^E_k$ is different from that for $\mathbf{Y}^E_k$. When the source is located in the elastic surface layer overlying a viscoelastic half-space, for example, the degree $M$of the polynomial is three for $\mathbf{Y}^E_k$ and one for $\mathbf{Y}'^E_k$. Given the explicit expressions for the rational functions, we can obtain the viscoelastic solution in the time domain by using the algorithm developed by Matsu'ura *et al.* (1981); that is, with division algorithm and partial fraction resolution, we can rewrite eq. (16) as

$$\tilde{\mathbf{Y}}^{(\prime)}_k(z,s;j) = \frac{1}{s}\mathbf{Y}^{(\prime)E}_k(z;j;\mu_l,\gamma_l) - \sum_{i=1}^M \mathbf{c}_i\left(\frac{1}{s} - \frac{1}{s-d_i}\right), \tag{21}$$

where

$$\mathbf{c}_i = \frac{1}{b^{(M)}d_i}\prod_{l=1(l\neq i)}^M \frac{1}{(d_i - d_l)}\sum_{l=0}^M \mathbf{a}^{(l)}d_i^l, \tag{22}$$

and d_i are the roots of the algebraic equation $\sum_{i=0}^M b^{(i)}s^i = 0$, which always take real negative values. Operation of the inverse Laplace transform on $\tilde{\mathbf{Y}}^{(\prime)}_k$ yields

$$\mathbf{Y}^{(\prime)}_k(z,t;j) = H(t)\left[\mathbf{Y}^{(\prime)E}_k(z;j;\mu_l,\gamma_l) - \sum_{i=1}^M \mathbf{c}_i\{1 - \exp(d_i t)\}\right]. \tag{23}$$

Finally, replacing $\tilde{\mathbf{Y}}^{(\prime)}_k(z,s;j)$ in eqs (14) and (15) with $\mathbf{Y}^{(\prime)}_k(z,t;j)$ in eq. (23), we obtain the viscoelastic displacement components u_i $(i = r, \varphi, z)$ and stress components σ_{zi} $(i = r, \varphi, z)$ in the time domain. When the jth layer is viscoelastic, we must also replace μ_j in eq. (15) with $\hat{\mu}_j$. In this case we can obtain the expressions for stress components $\sigma_{zi}(i = r, \varphi, z)$ in the time domain with additional partial fraction resolution.

From eq. (23) we can see that the viscoelastic solution consists of the instantaneous elastic deformation due to a dislocation source (the first term), and the viscoelastic transient deformation decaying with time (the second term). Here, it should be noted that the real negative roots d_i have strong wavenumber dependence (Matsu'ura *et al.* 1981), and so the viscoelastic transient deformation is expressed by the superposition of M modes with different wavenumber-dependent decay time functions. On the other hand, the completely relaxed viscoelastic solution $\mathbf{Y}_k^{(\prime)}(z;j;\, t\to\infty)$ is given by

$$\mathbf{Y}_k^{(\prime)}(z;\, j;\, t\to\infty) = \mathbf{Y}_k^{(\prime)E}(z;\, j;\, \mu_l,\, \gamma_l) - \sum_{i=1}^{M} \mathbf{c}_i = \frac{\mathbf{a}^{(0)}}{b^{(0)}}. \tag{24}$$

2.3 Derivation of the rational functions

In this subsection we give the algorithm to derive the explicit expressions for eq. (19). If the substratum is viscoelastic, using eq. (17), we can rewrite eq. (12) as

$$\begin{cases} \mathbf{Y}^E(z;\, j;\, \hat{\mu}_l,\, \hat{\gamma}_l) = \exp(-q\xi)\mathbf{S}_{jm}(z;\, \hat{\mu}_l,\, \hat{\gamma}_l) + \delta_{nj}\delta_{\mathrm{nm}}\exp(-|z-d|\,\xi)\big(s\mathbf{Y}^s(z;\, \gamma_n) + \kappa_n\mathbf{Y}^s(z;\, 1)\big)\big/(s+\kappa_n) \\ \mathbf{Y}'^E(z;\, j;\, \hat{\mu}_l) = \exp(-q\xi)\mathbf{S}'_{jm}(z;\, \hat{\mu}_l) + \delta_{nj}\delta_{\mathrm{nm}}\exp(-|z-d|\,\xi)\mathbf{Y}'^s(z), \end{cases} \tag{25}$$

otherwise

$$\begin{cases} \mathbf{Y}^E(z;\, j;\, \hat{\mu}_l,\, \hat{\gamma}_l) = \exp(-q\xi)\mathbf{S}_{jm}(z;\, \hat{\mu}_l,\, \hat{\gamma}_l) + \delta_{nj}\delta_{\mathrm{nm}}\exp(-|z-d|\,\xi)\mathbf{Y}^s(z;\, \gamma_n) \\ \mathbf{Y}'^E(z;\, j;\, \hat{\mu}_l) = \exp(-q\xi)\mathbf{S}'_{jm}(z;\, \hat{\mu}_l) + \delta_{nj}\delta_{\mathrm{nm}}\exp(-|z-d|\,\xi)\mathbf{Y}'^s(z). \end{cases} \tag{26}$$

Then, in order to obtain the expressions for $\mathbf{Y}_k^{(\prime)E}(z;\, j;\, \hat{\mu}_l,\, \hat{\gamma}_l)$ in the form of eq. (19), we need to rewrite the s-dependent factors $\mathbf{S}_{jm}^{(\prime)}(z;\, \hat{\mu}_l,\, \hat{\gamma}_l)$ in eq. (25) or (26) in a similar form to eq. (19), that is

$$\mathbf{S}_{jm}^{(\prime)}(z;\, \hat{\mu}_l,\, \hat{\gamma}_l) = \frac{\sum_{i=0}^{M}\mathbf{A}^{(\prime)(i)}s^i}{\sum_{i=0}^{M}B^{(\prime)(i)}s^i}. \tag{27}$$

As shown in the Appendix, both the numerator and the denominator of $\mathbf{S}_{jm}^{(\prime)}(z;\mu_l,\, \gamma_l)$ in the associated elastic solution are defined by the products of the matrices with the elements including the elastic constants, μ_l or γ_l, which are replaced by the corresponding s-dependent moduli in the viscoelastic solution. The formal expressions for the s-dependent matrices appearing in the numerator or denominator of $\mathbf{S}_{jm}^{(\prime)}(z;\, \hat{\mu}_l,\, \hat{\gamma}_l)$ are given by

$$\mathbf{F}(z;\, \hat{\gamma}_l) = \frac{1}{s+\kappa_l}\left(s\mathbf{F}(z;\, \gamma_l) + \kappa_l\mathbf{F}(z;\, 1)\right), \tag{28}$$

$$\mathbf{D}^{(\prime)}(\mu_{l-1},\, \hat{\mu}_l) = \frac{1}{s}\left(s\mathbf{D}^{(\prime)}(\mu_{l-1},\, \mu_l) + \frac{1}{\tau_l}\mathbf{D}_s^{(\prime)}(\mu_{l-1},\, \mu_l)\right), \tag{29}$$

$$\mathbf{D}^{(\prime)}(\hat{\mu}_l,\, \mu_{l+1}) = \frac{1}{s+1/\tau_l}\left(s\mathbf{D}^{(\prime)}(\mu_l,\, \mu_{l+1}) + \frac{1}{\tau_l}\mathbf{D}^{(\prime)}(0,\, \mu_{l+1})\right), \tag{30}$$

with

$$\mathbf{D}_s(\mu_{l-1},\, \mu_l) = \begin{pmatrix} 0 & 0 & 0 & 0 \\ 0 & 0 & 0 & 0 \\ 0 & 0 & \mu_{l-1}/\mu_l & 0 \\ 0 & 0 & 0 & \mu_{l-1}/\mu_l \end{pmatrix}, \quad \mathbf{D}'_s(\mu_{l-1},\, \mu_l) = \begin{pmatrix} 0 & 0 \\ 0 & \mu_{l-1}/\mu_l \end{pmatrix}, \tag{31}$$

if the viscoelastic layer intervenes between elastic layers. When the viscoelastic layer is adjacent to another viscoelastic layer, eqs (29) and (30) should be replaced by

$$\mathbf{D}^{(\prime)}(\hat{\mu}_l,\, \hat{\mu}_{l+1}) = \frac{1}{s+1/\tau_l}\left(s\mathbf{D}^{(\prime)}(\mu_l,\, \mu_{l+1}) + \frac{1}{\tau_l}\mathbf{D}^{(\prime)}(\eta_l,\, \eta_{l+1})\right). \tag{32}$$

In addition to these, if the source is located in the viscoelastic layer, the following s-dependent matrix appears in the numerator of $\mathbf{S}_{jm}(z;\, \hat{\mu}_l,\, \hat{\gamma}_l)$:

$$\mathbf{\Delta}(\hat{\gamma}_m) = \frac{1}{s+\kappa_m}\left(s\mathbf{\Delta}(\gamma_m) + \kappa_m\mathbf{\Delta}(1)\right). \tag{33}$$

If the substratum is viscoelastic, we use

$$\mathbf{E}(z;\, \hat{\gamma}_n) = \frac{1}{s+\kappa_n}\left(s\mathbf{E}(z;\, \gamma_n) + \kappa_n\mathbf{E}(z;\, 1)\right). \tag{34}$$

The explicit expressions for $\mathbf{F}$, $\mathbf{D}^{(\prime)}$, $\mathbf{\Delta}$ and $\mathbf{E}$ are given in the Appendix. Here, it should be noted that all the s-dependent matrices in eqs (28)–(30) and (32)–(34) have the form of a rational function of first-degree polynomials in s. The product of two polynomials can generally be calculated with the following rule:

$$\sum_{i=0}^{n_1}a^{(i)}s^i\sum_{j=0}^{n_2}b^{(j)}s^j = \sum_{p=0}^{n_1+n_2}c^{(p)}s^p, \tag{35}$$

where

$$c^{(p)} = \sum_{k=I}^{E} a^{(p-k)} b^{(k)}, \tag{36}$$

with

$$\begin{cases} I = 0 & (p \le n_1) \\ I = p - n_1 & (p > n_1), \end{cases} \quad \begin{cases} E = p & (p \le n_2) \\ E = n_2 & (p > n_2). \end{cases} \tag{37}$$

Here, $a^{(i)}$ and $b^{(i)}$ may be vectors or matrices. Therefore, applying the rule in eq. (35) to the numerator and to the denominator of $\mathbf{S}^{(\prime)}_{jm}(z; \hat{\mu}_l, \hat{\gamma}_l)$ repeatedly, we can obtain the expressions for $\mathbf{S}^{(\prime)}_{jm}(z; \hat{\mu}_l, \hat{\gamma}_l)$ in the form of eq. (27).

3 EQUIVALENCE THEOREM

The quasi-static deformation field due to a dislocation source tends to a certain steady state with the progress of stress relaxation in viscoelastic layers. In some problems we are not interested in the process of stress relaxation, but in the steady state after complete relaxation. In this section we show that the completely relaxed viscoelastic solution can be obtained directly from the associated elastic solution without passing through the complicated viscoelastic calculation described in the previous section.

With the limiting value theorem of the Laplace transform we can directly evaluate the ultimate displacement field u_i at $t \to \infty$ from the viscoelastic solution $\tilde{u}_i$ in the s-domain as

$$\lim_{t\to\infty} u_i(r, \varphi, z, t; j) = \lim_{s\to 0} s\tilde{u}_i(r, \varphi, z, s; j). \tag{38}$$

On the basis of the correspondence principle, as shown in eqs (7), (14) and (16), we can express the viscoelastic step response in the s-domain in terms of the associated elastic response as

$$\tilde{u}_i(r, \varphi, z, s; j) = \frac{1}{s} u_i^E(r, \varphi, z, t > 0; j; \hat{\mu}_l, \hat{\gamma}_l). \tag{39}$$

Here, we assumed that only one layer is viscoelastic, for simplicity. Substituting eq. (39) into eq. (38), we obtain

$$\lim_{t\to\infty} u_i(r, \varphi, z, t; j) = \lim_{s\to 0} u_i^E(r, \varphi, z, t > 0; j; \hat{\mu}_l, \hat{\gamma}_l). \tag{40}$$

Using the explicit expressions for $\hat{\mu}_l(s)$ in eq. (4) and $\hat{\gamma}_l(s)$ in eq. (17), we can obtain the limiting values of the s-dependent moduli $\hat{\mu}_l(s)$ and $\hat{\gamma}_l(s)$ at $s \to 0$ as

$$\lim_{s\to 0} \hat{\mu}_l(s) = 0, \quad \lim_{s\to 0} \hat{\gamma}_l(s) = 1. \tag{41}$$

Then, we may rewrite eq. (40) as

$$\lim_{t\to\infty} u_i(r, \varphi, z, t; j) = u_i^E(r, \varphi, z, t > 0; j; \mu_l \to 0, 1). \tag{42}$$

In the same way, we can obtain the following parallel relations for stress and strain components:

$$\lim_{t\to\infty} \sigma_{ij}(r, \varphi, z, t; j) = \sigma_{ij}^E(r, \varphi, z, t > 0; j; \mu_l \to 0, 1), \tag{43}$$

and

$$\lim_{t\to\infty} \varepsilon_{ij}(r, \varphi, z, t; j) = \varepsilon_{ij}^E(r, \varphi, z, t > 0; j; \mu_l \to 0, 1). \tag{44}$$

Based on eq. (24), we can confirm the validity of eqs (42)–(44) from the direct calculation described in the previous section.

Eqs (42)–(44) mean that the viscoelastic step response at $t \to \infty$ is mathematically equivalent to the associated elastic response with $\mu_l \to 0$ and $\gamma_l = 1$. In other words, the viscoelastic medium cannot support any deviatoric stress at $t \to \infty$. Here, we should note that the completely relaxed solution does not depend on the value of viscosity, which just controls the speed of viscous relaxation. Hereafter, we refer to the theoretical relation described by eqs (42)–(44) as the 'equivalence theorem' in linear viscoelastic problems.

If we take the elastic constants (μ_l, K_l) or (μ_l, λ_l) instead of (μ_l, γ_l) to express the deformation fields, we obtain other expressions for the equivalence theorem. Denoting the viscoelastic step response by $\mathbf{q}(t; \mu_l, K_l)$ or $\mathbf{q}'(t; \mu_l, \lambda_l)$ and the associated elastic response by $\mathbf{q}^E(t; \mu_l, K_l)$ or $\mathbf{q}'^E(t; \mu_l, \lambda_l)$, we obtain

$$\lim_{t\to\infty} \mathbf{q}(t; \mu_l, K_l) = \mathbf{q}^E(t > 0; \mu_l \to 0, K_l), \tag{45}$$

Table 1. Two-layer structure model used for the computations in Section 4.

No.	H (km)	V_p (km s^{-1})	V_s (km s^{-1})	ρ (kg m^{-3})
1	30	6.0	3.5	2.6×10^3
2	∞	8.0	4.5	3.4×10^3

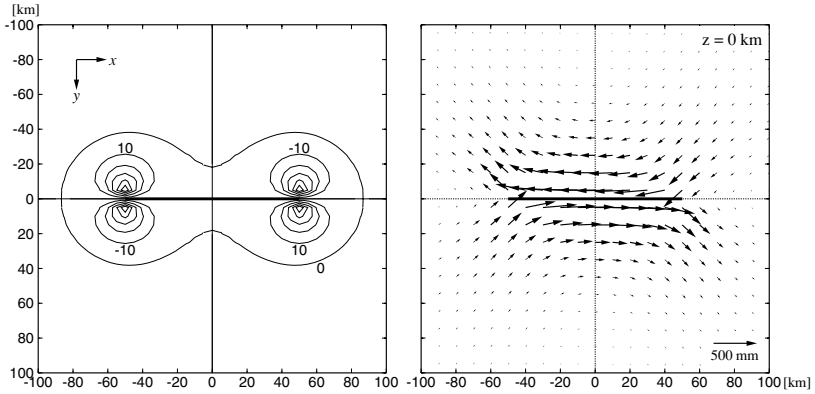

Figure 2. Coseismic vertical (left) and horizontal (right) surface displacements due to unit (1 m) left-lateral strike-slip displacement on a vertical fault in an elastic surface layer overlying a viscoelastic half-space. The fault length is taken to be 100 km ($x = -50$ to 50 km), and the fault width to be 30 km ($z = 0$ to 30 km), which is the same as the thickness of the elastic surface layer. The structural parameters are given in Table 1. The contour interval of the vertical displacement is 10 mm, and the uplift is taken to be positive.

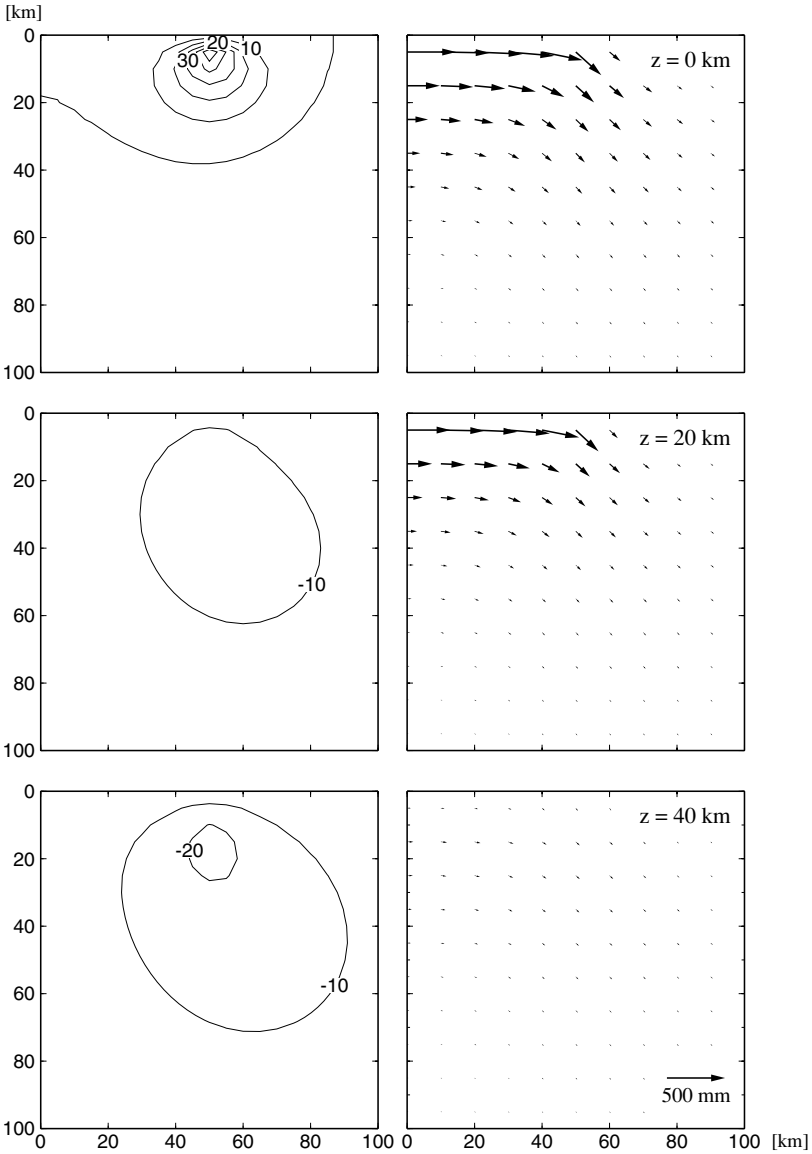

Figure 3. Variation of the coseismic displacement fields with depth. The vertical and horizontal components in the fourth quadrant at $z = 0$, 20 and 40 km are shown in the left and right columns, respectively. See Fig. 2 caption for fault model and structural parameters. The contour interval of the vertical displacement is 10 mm, and uplift is taken to be positive.

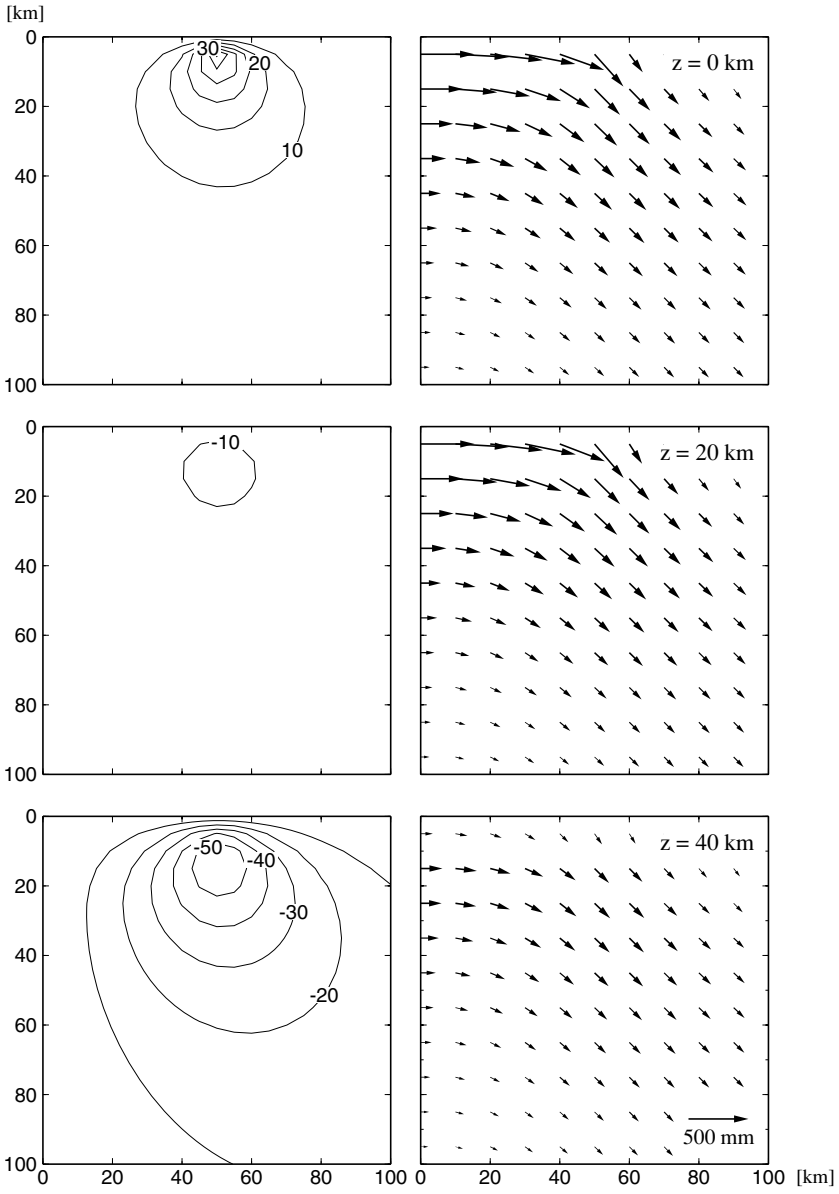

Figure 4. Variation of the completely relaxed viscoelastic displacement fields with depth. The vertical and horizontal components in the fourth quadrant at $z = 0$, 20 and 40 km are shown in the left and right columns, respectively. See Fig. 2 caption for fault model and structural parameters. The contour interval of the vertical displacement is 10 mm, and uplift is taken to be positive.

or

$$\lim_{t\to\infty} \mathbf{q}'(t;\mu_l,\lambda_l) = \mathbf{q}'^{E}(t>0;\mu_l\to 0, K_l). \tag{46}$$

Here, we used

$$\lim_{s\to 0} \hat{\lambda}_l(s) = K_l. \tag{47}$$

When the half-space contains more than one Maxwell viscoelastic layer with different viscosities, we need to pay special attention to taking the limit $\mu_l \to 0$, because the relaxation speed in each layer depends on its viscosity. As an example, let's consider a half-space with two Maxwell viscoelastic layers, (μ_i, K_i, η_i) and (μ_j, K_j, η_j). In this case the equivalence theorem is expressed as

$$\lim_{t\to\infty} \mathbf{q}(t;\mu_i,K_i,\mu_j,K_j) = \mathbf{q}^{E}(t>0;\mu_i\to 0, K_i, \mu_j\to 0, K_j), \tag{48}$$

but the limit $\mu_i \to 0$ and $\mu_j \to 0$ must be taken under the following condition:

$$\frac{\mu_i}{\mu_j} = \frac{\eta_i}{\eta_j}. \tag{49}$$

Thus, the completely relaxed viscoelastic solution depends on the ratio of viscosities η_i/η_j.

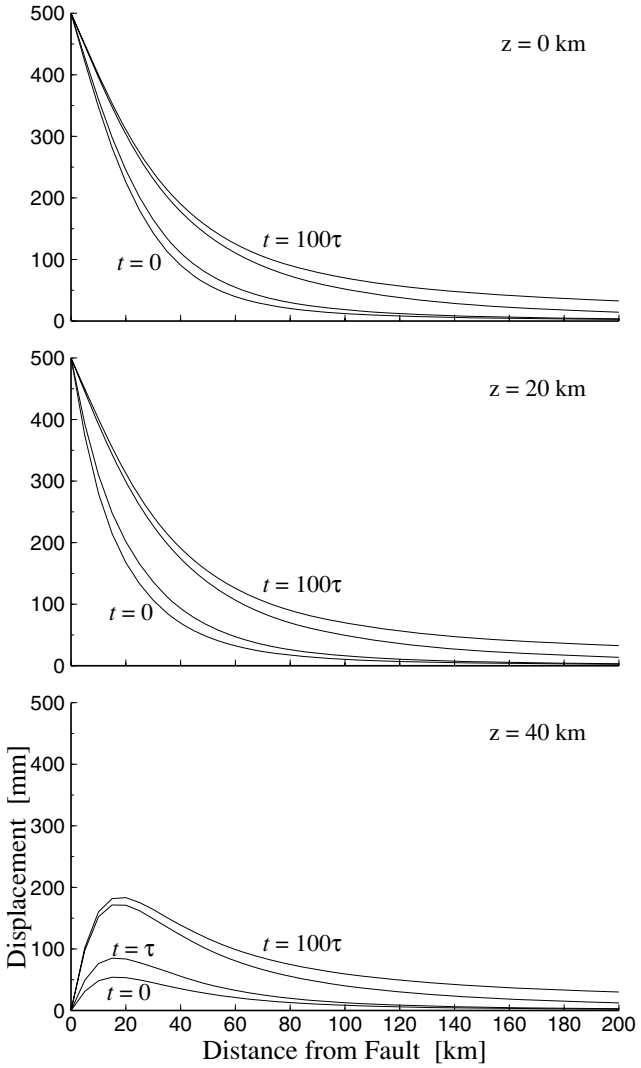

Figure 5. Temporal variation of fault-parallel displacements on the y-axis. The four curves in each diagram show the displacement profiles at $t = 0, \tau, 10\tau$ and 100τ from bottom to top, respectively. Here, τ is the Maxwell relaxation time of the viscoelastic substratum defined in eq. (5) of the text. See Fig. 2 caption for fault model and structural parameters.

In the present study we assumed Maxwell viscoelasticity. When a medium has isotropic linear viscoelasticity, we can express the equivalence theorem as

$$\lim_{t\to\infty} \mathbf{q}(t; \mu_l, K_l) = \mathbf{q}^E\left(t > 0; \mu_l^\infty, K_l^\infty\right), \tag{50}$$

with

$$\mu_l^\infty = \lim_{s\to 0} \hat{\mu}_l(s), \quad K_l^\infty = \lim_{s\to 0} \hat{K}_l(s). \tag{51}$$

Here, $\hat{\mu}_l(s)$ and $\hat{K}_l(s)$ are the Laplace operators for the linear viscoelastic medium considered.

In the derivation of the equivalence theorem, we only used the correspondence principle of linear viscoelasticity, the limiting value theorem of the Laplace transform, and the constitutive equations of viscoelastic media. Therefore, we may apply the equivalence theorem not only to the stratified elastic-viscoelastic medium but also to general elastic and linear-viscoelastic composite media. Incidentally, we can regard the equivalence theorem as a particular case of the Tauberian theorem for the Laplace transform.

4 NUMERICAL EXAMPLES

On the basis of the mathematical expressions derived in Section 2, we developed a computer program to calculate the internal viscoelastic deformation fields due to faulting. In order to obtain the deformation fields due to a finite-dimensional fault, we numerically integrate the solutions for point dislocation sources over a fault surface. Usually it is not difficult to obtain results around the accuracy of 1 per cent, in comparison with the analytical solution for an elastic half-space. Our semi-analytical solution has singular points at the depth $z = d$. From

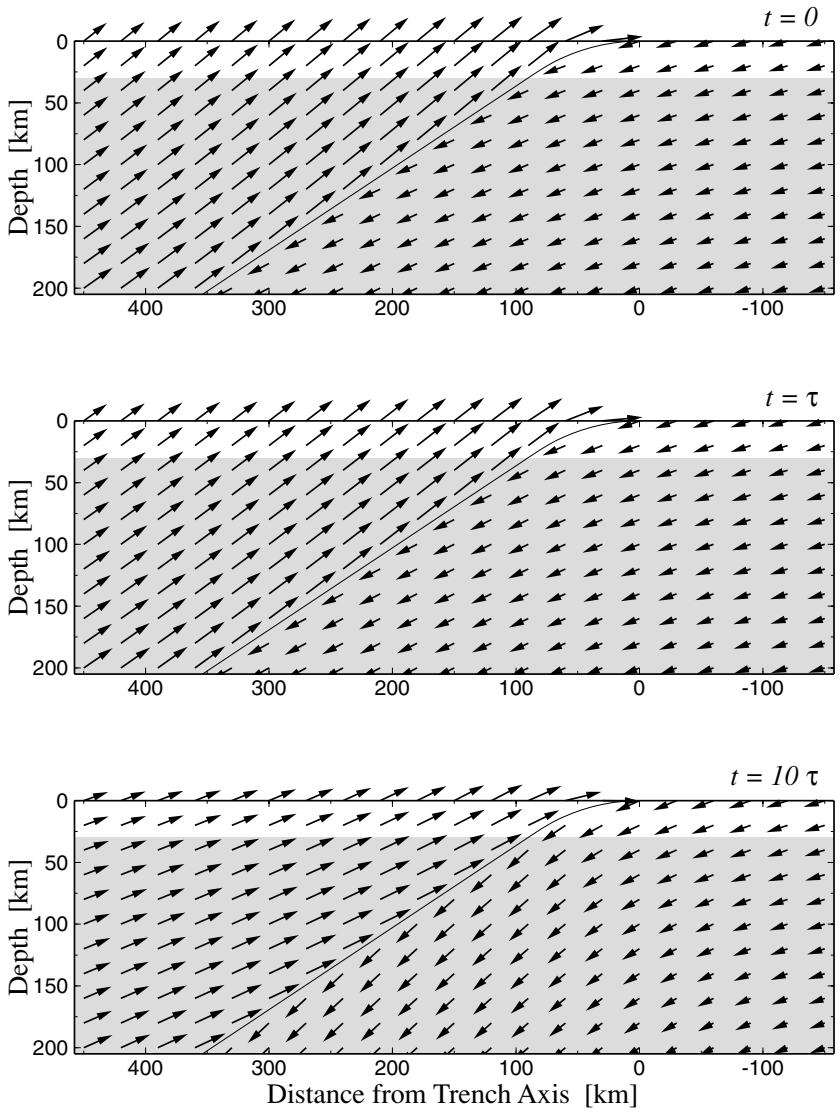

Figure 6. Temporal change of the viscoelastic displacement field due to uniform (1 m) dip-slip displacement at $t = 0$ on a curved plate interface that divides the layered elastic-viscoelastic half-space into two blocks. The structural parameters are given in Table 1. The plate interface, indicated by the thin solid line in each diagram, extends to a depth of 600 km and infinitely in the direction parallel to its strike without changing the geometry. In each diagram the centre of mass of the total system is taken as the fixed point to measure the displacements.

the continuity condition of displacement and stress, however, we obtain

$$\begin{cases} \lim_{z\to d-} u_i(r,\varphi,z) = \lim_{z\to d+} u_i(r,\varphi,z) \\ \lim_{z\to d-} \sigma_{zi}(r,\varphi,z) = \lim_{z\to d+} \sigma_{zi}(r,\varphi,z) \end{cases} (i = r,\varphi,z), \tag{52}$$

except for the points on the dislocation source itself, and so we can avoid the singularity problem by substituting $z = d + \varepsilon$ for $z = d$ in the computation of deformation fields, where ε represents a small value. In the following part of this section we show some numerical examples obtained by the computer program. If our interest is limited to the completely relaxed solution, we can use the elastic solution (Fukahata & Matsu'ura 2005) instead of the viscoelastic solution, owing to the equivalence theorem.

First, we consider the case of unit (1 m) strike-slip motion on a vertical fault in an elastic surface layer overlying a viscoelastic half-space. The fault length is taken to be 100 km ($x = -50$ to 50 km), and the fault width to be 30 km ($z = 0$ to 30 km), which is the same as the thickness of the elastic surface layer. The values of the structural parameters used for the computation are given in Table 1. In Fig. 2 we show the vertical (left) and horizontal (right) surface displacements at $t = 0$. Here, the contour interval of the vertical displacement is 10 mm, and the uplift is taken to be positive. In the case of vertical strike slip, as can be seen from Fig. 2, the displacement fields at any depth z have good symmetry about the point $(0, 0, z)$. So, in Figs 3 and 4, we show the displacement fields only in the fourth quadrant. The variation of the coseismic displacement fields with depth is shown in Fig. 3. We can see from Fig. 3 that the coseismic displacement rapidly decreases with depth.

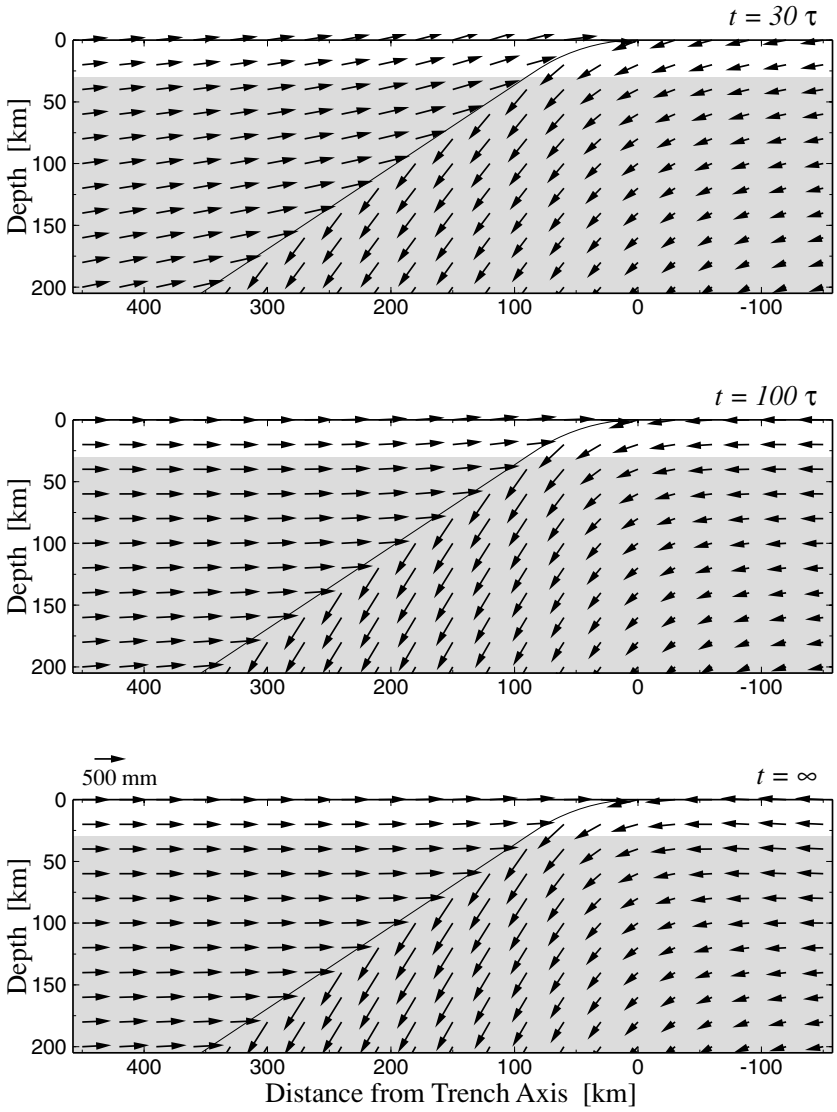

Figure 6. (*Continued.*)

In Fig. 4 we show the displacement fields at $t = \infty$. Based on the equivalence theorem, we can calculate the same displacement field as in Fig. 4 with the computer program for elastic displacements by replacing only the value of *S*-wave velocity in the substratum with a very small value. The displacements at $t = \infty$ in Fig. 4 are much larger than the displacements at $t = 0$ in Fig. 3 particularly in the far field. This is the effect of stress relaxation in the viscoelastic substratum. Furthermore, we should note that the pattern of horizontal components (right column) at $t = \infty$ does not change within the elastic surface layer ($z = 0$ to 30 km), while the vertical components (left column) show a symmetric pattern with respect to the horizontal plane at $z = 15$ km. These features of the displacement field at $t = \infty$ can be intuitively understood from the equivalence theorem; that is, after the completion of stress relaxation in the viscoelastic substratum, the surface layer behaves just like an elastic plate floating on water, because the viscoelastic substratum cannot support any deviatoric stress at $t = \infty$.

In Fig. 5 we show the temporal variation of fault-parallel displacements on the y-axis at $t/\tau = 0$, 1, 10 and 100. Here, τ is the Maxwell relaxation time of the viscoelastic substratum, defined by eq. (5). From Fig. 5 we can see that rapid variation of fault-parallel displacements occurs during the period from $t/\tau = 1$ to 10. The displacement profile at $t/\tau = 100$ is almost identical to that at $t = \infty$ (they look the same on the graph).

The next numerical example is the internal displacement field due to mechanical interaction at a subduction-zone plate interface. As demonstrated in a series of papers by Matsu'ura and his coworkers (Matsu'ura & Sato 1989, 1997; Sato & Matsu'ura 1988, 1992; Hashimoto & Matsu'ura 2000, 2002; Takada & Matsu'ura 2004), we can rationally represent mechanical interaction at a plate interface by the increase of tangential displacement discontinuity (fault slip) across it. So, in computation, we consider the case of uniform (1 m) dip-slip motion at $t = 0$ on a curved plate interface that divides the layered elastic-viscoelastic half-space into two blocks. Here, we use the same structural parameters as given in Table 1. In Fig. 6 we show the temporal change of the viscoelastic internal displacement field from $t = 0$ to ∞ together with the geometry of the plate interface (thin solid line in each diagram). Here, the curved plate interface extends to a depth of 600 km and infinitely

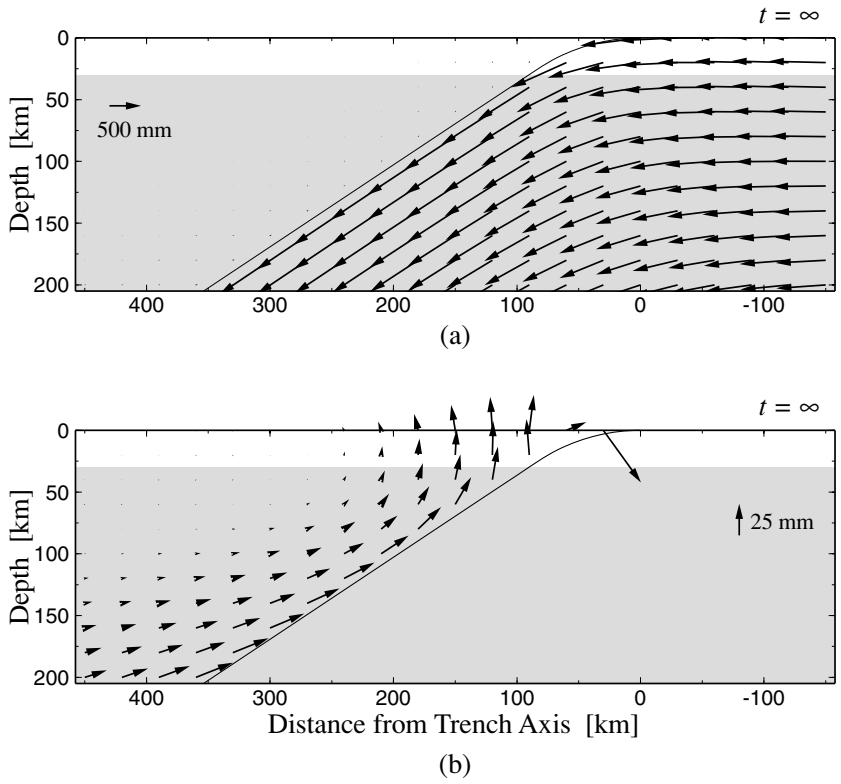

Figure 7. Different representation of the completely relaxed viscoelastic displacement field due to uniform (1 m) dip-slip motion over the whole plate interface. A point distant from the plate interface on the hangingwall side is taken as the fixed point to measure the displacements. The geometry of the plate interface is as in Fig. 6, and the structural parameters are given in Table 1. (a) The total displacement field. The displacements of the hangingwall block are very small, but not completely zero. (b) The displacement field of the hangingwall block, magnified 20 times.

in the direction parallel to its strike without changing the geometry. In such a case we can use the solution for a line source instead of that for a point source. The explicit expressions for a line dislocation source can be directly obtained from those for a point dislocation source by replacing the z-independent vectors, $\mathbf{J}$ and $\mathbf{J}'$, in eq. (9) with the corresponding vectors, $\mathbf{b}'_x$, $\mathbf{b}_y$ and $\mathbf{b}_z$, in eq. (63) of Fukahata & Matsu'ura (2005). The displacement fields at $t = 0$ and τ (the first two diagrams of Fig. 6) show a large uplift of the hangingwall block and a small subsidence of the footwall block. On the other hand, the displacement fields at $t = 100\tau$ and ∞ (the last two diagrams) are characterized by a horizontal convergence of the two blocks. The transition from the first instantaneous elastic response to the ultimate viscoelastic response, caused by the stress relaxation in the viscoelastic substratum under gravity, are shown in the middle two diagrams ($t = 10\tau$ and 30τ). Here, it should be noted that the centre of mass of the total system does not move in this computation except for the effect of gravity, and so we take it as the fixed point to measure the displacements.

In Fig. 7(a) we show the internal displacement field at $t = \infty$ again, but taking a point distant from the plate interface on the hangingwall side as the fixed point. In this more familiar representation, the displacements of the hangingwall block become very small, but not completely zero. In order to see the deformation field of the hangingwall block we magnify the displacement vectors 20 times in Fig. 7(b). The displacement fields in Fig. 7 are the completely relaxed viscoelastic response to a unit step slip over the whole plate interface. As demonstrated by Matsu'ura & Sato (1989) and Sato & Matsu'ura (1993) on the basis of the method of hereditary integral, however, the completely relaxed viscoelastic step-response gives the deformation rate due to a steady slip for sufficiently large time ($t \gg \tau$). That is to say, we can read the displacement fields at $t = \infty$ in Fig. 7 as the long-term velocity fields due to a steady slip over the whole plate interface. From Fig. 7(a) we can see that the steady subduction of an oceanic plate is realized by giving the steady increase of tangential displacement discontinuity across the plate interface. From Fig. 7(b), on the other hand, we can see that the steady plate subduction brings about the steady subsidence of ocean trenches and the steady uplift of island arcs (Sato & Matsu'ura 1988, 1993). Furthermore, the steady uplift of island arcs induces upward motion in mantle wedges. In actual situations, however, such upward motion may largely be affected by thermal convection in mantle wedges.

5 DISCUSSION AND CONCLUSIONS

We obtained general expressions for quasi-static internal deformation fields due to a dislocation source in a multilayered elastic/viscoelastic half-space under gravity by applying the correspondence principle of linear viscoelasticity to the associated elastic solution derived by Fukahata & Matsu'ura (2005). The difficulty in obtaining the viscoelastic solution in the time domain is to perform the inverse Laplace transform for the s-dependent solution. For example, Rundle and his colleagues (Rundle 1978, 1982; Yu *et al.* 1996; Fernández *et al.* 1996) have introduced

an approximation technique to perform the inverse Laplace transform. In the present study we developed a systematic approach to the inverse Laplace transform without approximation by repeatedly applying the rule of the product of two polynomials together with the algorithm developed by Matsu'ura *et al.* (1981).

The viscoelastic step response at $t = \infty$ is equivalent to the associated elastic response obtained by taking the rigidity of the elastic medium corresponding to a Maxwell viscoelastic layer or substratum to be zero. In Section 3 we gave an explicit mathematical proof of this theoretical relationship, named the 'equivalence theorem' in linear viscoelastic problems, on the basis of the correspondence principle of linear viscoelasticity and the limiting value theorem of the Laplace transform. The equivalence theorem is applicable not only to the stratified elastic-viscoelastic medium but also to general elastic and linear-viscoelastic composite media. Owing to the equivalence theorem, we can obtain the completely relaxed viscoelastic solution directly from the associated elastic solution without passing through the complicated viscoelastic calculation. Furthermore, the equivalence theorem enables us to check the complicated computation code for viscoelastic deformation not only at $t = 0$ (elastic solution) but also at $t = \infty$ by using a simple code for elastic deformation.

The inherent stress relaxation time of a viscoelastic medium is given by the Maxwell relaxation time τ, defined in eq. (5). As shown through the numerical computations in Section 4, however, the effective stress relaxation time of the elastic-viscoelastic total system is much longer than the Maxwell relaxation time τ. If we take the viscosity of the viscoelastic substratum to be 10^{19} Pa s, the Maxwell relaxation time τ is about 5 yr, but the effective stress relaxation time of the total system can be 100 yr or more.

ACKNOWLEDGMENTS

We would like to thank Toshinori Sato, Akinori Hashima, Isabelle Ryder and Ernian Pan for their useful comments. We also thank anonymous reviewers.

REFERENCES

Barr, T.D. & Dahlen, F.A., 1989. Brittle frictional mountain building 2. Thermal structure and heat budget, *J. geophys. Res.,* **94,** 3923–3947.

Cohen, C., 1980a. Postseismic viscoelastic surface deformation and stress, 1. Theoretical considerations, displacement, and strain calculations, *J. geophys. Res.,* **85,** 3131–3150.

Cohen, C., 1980b. Postseismic viscoelastic surface deformation and stress, 2. Stress theory and computation; dependence of displacement, strain and stress on fault parameters, *J. geophys. Res.,* **85,** 3151–3158.

England, P.C. & Thompson, A.B., 1984. Pressure-temperature-time paths of regional metamorphism I. Heat transfer during the evolution of regions of thickened continental crust, *J. petrol.,* **25,** 894–928.

Fernández, J., Yu, T.T. & Rundle, J.B., 1996. Horizontal viscoelastic-gravitational displacement due to a rectangular dipping thrust fault in a layered Earth model, *J. geophys. Res.,* **101,** 13581–13594.

Fukahata, Y. & Matsu'ura, M., 2000. Effects of active crustal movements on thermal structure in subduction zones, *Geophys. J. Int.,* **141,** 271–281.

Fukahata, Y. & Matsu'ura, M., 2005. General expressions for internal deformation fields due to a dislocation source in a multilayered elastic half-space, *Geophys. J. Int.,* **161,** 507–521.

Fukahata, Y., Nishitani, A. & Matsu'ura, M., 2004. Geodetic data inversion using ABIC to estimate slip history during one earthquake cycle with viscoelastic slip-response functions, *Geophys. J. Int.,* **156,** 140–153.

Hashimoto, C., Fukui, K. & Matsu'ura, M., 2004. 3-D modelling of plate interfaces and numerical simulation of long-term crustal deformation in and around Japan, *Pure Appl. Geophys.,* **161,** 2053–2068.

Hashimoto, C. & Matsu'ura, M., 2000. 3-D physical modelling of stress accumulation processes at transcurrent plate boundaries, *Pure Appl. Geophys.,* **157,** 2125–2147.

Hashimoto, C. & Matsu'ura, M., 2002. 3-D simulation of earthquake generation cycles and evolution of fault constitutive properties, *Pure Appl. Geophys*. **159,** 2175–2199.

Iwasaki, T. & Matsu'ura, M., 1981. Quasi-static strain and tilt due to faulting in a layered half-space with an intervenient viscoelastic layer, *J. Phys. Earth,* **29,** 499–518.

Jovanovich, D.B., Husseini, M.I. & Chinnery, M.A., 1974. Elastic dislocations in a layered half-space—I. Basic theory and numerical methods, *Geophys. J. R. astr. Soc.,* **39,** 205–217.

Lee, E.H., 1955. Stress analysis in visco-elastic bodies, *Q. Appl. Math.,* **13,** 183–190.

Ma, X.Q. & Kusznir, N.J., 1992. 3-D subsurface displacement and strain fields for faults and fault arrays in a layered elastic half space, *Geophys. J. Int.,* **111,** 542–558.

Ma, X.Q. & Kusznir, N.J., 1994a. Effects of rigidity layering, gravity and stress relaxation on 3-D subsurface fault displacement fields, *Geophys. J. Int.,* **118,** 201–220.

Ma, X.Q. & Kusznir, N.J., 1994b. Coseismic and postseismic subsurface displacements and strains for a vertical strike-slip fault in a three-layer elastic medium, *Pure Appl. Geophys.,* **142,** 687–709.

Ma, X.Q. & Kusznir, N.J., 1995. Coseismic and postseismic subsurface displacements and strains for a dip-slip normal fault in a three-layer elastic-gravitational medium, *J. geophys. Res.,* **100,** 12 813–12 828.

Matsu'ura, M., 2005. Quest for predictability of geodynamic processes through computer simulation, *Computing in Science &Engineering,* **7,** 43–50.

Matsu'ura, M. & Iwasaki, T., 1983. Study on coseismic and postseismic crustal movements associated with the 1923 Kanto earthquake, *Tectonophysics,* **97,** 201–215.

Matsu'ura, M. & Sato, T., 1989. A dislocation model for the earthquake cycle at convergent plate boundaries, *Geophys. J. Int.,* **96,** 23–32.

Matsu'ura, M. & Sato, T., 1997. Loading mechanism and scaling relations of large interplate earthquakes, *Tectonophysics,* **277,** 189–198.

Matsu'ura, M., Tanimoto, T. & Iwasaki, T., 1981. Quasi-static displacements due to faulting in a layered half-space with an intervenient viscoelastic layer, *J. Phys. Earth,* **29,** 23–54.

Pan, E., 1989. Static response of a transversely isotropic and layered half-space to general dislocation sources, *Phys. Earth Planet. Inter.,* **58,** 103–117.

Pan, E., 1997. Static Green's functions in multilayered half spaces, *Appl. Math. Modelling,* **21,** 509–521.

Radok, J.R.M., 1957. Visco-elastic stress analysis, *Q. Appl. Math.,* **15,** 198–202.

Rundle, J.B., 1978. Viscoelastic crustal deformation by finite quasi-static sources, *J. geophys. Res.,* **83,** 5937–5945.

Rundle, J.B., 1982. Viscoelastic-gravitational deformation by a rectangular thrust fault in a layered earth, *J. geophys. Res.,* **87,** 7787–7796.

Sato, R., 1971. Crustal deformation due to dislocation in a multi-layered medium, *J. Phys. Earth,* **19,** 31–46.

Sato, T. & Matsu'ura, M., 1988. A kinematic model for deformation of the lithosphere at subduction zones, *J. geophys. Res.,* **93,** 6410–6418.

Sato, T. & Matsu'ura, M., 1992. Cyclic crustal movement, steady uplift of marine terraces, and evolution of the island arc-trench system in southwest Japan, *Geophys. J. Int.,* **111,** 617–629.

Sato, T. & Matsu'ura, M., 1993. A kinematic model for evolution of island arc-trench systems, *Geophys. J. Int.,* **114,** 512–530.

Singh, S.J., 1970. Static deformation of a multilayered half-space by internal sources, *J. geophys. Res.,* **75,** 3257–3263.

Stuart, W.D., 1988. Forecast model for great earthquakes at the Nankai trough subduction zone, *Pure Appl. Geophys.,* **126,** 619–641.

Takada, Y. & Matsu'ura, M., 2004. A unified interpretation of vertical movement in Himalaya and horizontal deformation in Tibet on the basis of elastic and viscoelastic dislocation theory, *Tectonophysics,* **383,** 105–131.

Thatcher, W. & Rundle, J.B., 1984. A viscoelastic coupling model for the cyclic deformation due to periodically repeated earthquakes at subduction zones, *J. geophys. Res.,* **89,** 7631–7640.

Tse, S.T. & Rice, J.R., 1986. Crustal earthquake instability in relation to the depth variation of frictional slip properties, *J. geophys. Res.,* **91,** 9452–9472.

Yu, T.T., Rundle, J.B. & Fernández, J., 1996. Surface deformation due to a strike-slip fault in an elastic gravitational layer overlying a viscoelastic gravitational half-space, *J. geophys. Res.,* **101,** 3199–3214.

APPENDIX: EXPLICIT EXPRESSIONS FOR $\mathbf{S}_{jm}^{(\prime)}$ AND $\mathbf{Y}^{(\prime)s}$

Explicit expressions for $\mathbf{S}_{jm}^{(\prime)}(z;\mu_l, \gamma_l)$ are given as follows:

(i) $j \neq n$ and $z < d$:

$$\mathbf{S}_{jm}(z;\mu_l,\gamma_l) = \frac{\mathbf{R}_j(z)\mathbf{V}_m}{\delta}, \quad \mathbf{S}'_{jm}(z;\mu_l,\gamma_l) = \frac{\mathbf{R}'_j(z)\mathbf{V}'_m}{\delta'}, \tag{A1}$$

where

$$\begin{cases} \mathbf{R}_j(z) = \mathbf{F}(z-H_{j-1};\gamma_j)\prod_{l=1}^{j-1}[\mathbf{D}(\mu_{j-l},\mu_{j-l+1})\mathbf{F}(h_{j-l};\gamma_{j-l})]\mathbf{G}(\mu_1) \\ \mathbf{R}'_j(z) = \mathbf{F}'(z-H_{j-1})\prod_{l=1}^{j-1}[\mathbf{D}'(\mu_{j-l},\mu_{j-l+1})\mathbf{F}'(h_{j-l})], \end{cases} \tag{A2}$$

$$\mathbf{V}_m = \begin{pmatrix} (P_{22}+P_{42})\left(\mathbf{Q}_1^m+\mathbf{Q}_3^m\right)-(P_{12}+P_{32})\left(\mathbf{Q}_2^m+\mathbf{Q}_4^m\right) \\ -(P_{21}+P_{41})\left(\mathbf{Q}_1^m+\mathbf{Q}_3^m\right)+(P_{11}+P_{31})\left(\mathbf{Q}_2^m+\mathbf{Q}_4^m\right) \\ \mathbf{0} \\ \mathbf{0} \end{pmatrix}, \quad \mathbf{V}'_m = \begin{pmatrix} \mathbf{Q}_1'^m+\mathbf{Q}_2'^m \\ \mathbf{0} \end{pmatrix}, \tag{A3}$$

$$\delta = (P_{11}+P_{31})(P_{22}+P_{42})-(P_{12}+P_{32})(P_{21}+P_{41}), \quad \delta' = P'_{11}+P'_{21}, \tag{A4}$$

with

$$\mathbf{P} = \mathbf{E}^{-1}(0;\gamma_n)\prod_{j=1}^{n-1}[\mathbf{D}(\mu_{n-j},\mu_{n-j+1})\mathbf{F}(h_{n-j};\gamma_{n-j})]\mathbf{G}(\mu_1), \quad \mathbf{P}' = \prod_{j=1}^{n-1}[\mathbf{D}'(\mu_{n-j},\mu_{n-j+1})\mathbf{F}'(h_{n-j})], \tag{A5}$$

$$\begin{cases} \mathbf{Q}^m = \begin{cases} \mathbf{E}^{-1}(0;\gamma_n)\prod_{j=1}^{n-m-1}\left[\mathbf{D}(\mu_{n-j},\mu_{n-j+1})\mathbf{F}(h_{n-j};\gamma_{n-j})\right]\mathbf{D}(\mu_m,\mu_{m+1})\mathbf{F}(H_m-d;\gamma_m)\boldsymbol{\Delta}(\gamma_m) & (m\neq n) \\ \mathbf{E}^{-1}(0;\gamma_n)\mathbf{Y}^s(H_{n-1};\gamma_n) & (m=n) \end{cases} \\ \mathbf{Q}'^m = \begin{cases} \prod_{j=1}^{n-m-1}[\mathbf{D}'(\mu_{n-j},\mu_{n-j+1})\mathbf{F}'(h_{n-j})]\mathbf{D}'(\mu_m,\mu_{m+1})\mathbf{F}'(H_m-d)\boldsymbol{\Delta}' & (m\neq n) \\ \mathbf{Y}'^s(H_{n-1}) & (m=n). \end{cases} \end{cases} \tag{A6}$$

(ii) $j = n$ or $z > d$:

$$\mathbf{S}_{jm}(z;\mu_l,\gamma_l) = \frac{\bar{\mathbf{R}}_j(z)\bar{\mathbf{V}}_m}{\bar{\delta}}, \quad \mathbf{S}'_{jm}(z;\mu_l,\gamma_l) = \frac{\bar{\mathbf{R}}'_j(z)\bar{\mathbf{V}}'_m}{\bar{\delta}'}, \tag{A7}$$

where

$$\begin{cases} \bar{\mathbf{R}}_j(z) = \begin{cases} \mathbf{F}(z-H_j;\gamma_j)\mathbf{D}(\mu_{j+1},\mu_j)\prod_{l=j+1}^{n-1}[\mathbf{F}(-h_l;\gamma_l)\mathbf{D}(\mu_{l+1},\mu_l)]\mathbf{E}(0;\gamma_n) & (j\neq n) \\ \mathbf{E}(z-H_{n-1};\gamma_n) & (j=n) \end{cases} \\ \bar{\mathbf{R}}'_j(z) = \begin{cases} \mathbf{F}'(z-H_j)\mathbf{D}'(\mu_{j+1},\mu_j)\prod_{l=j+1}^{n-1}[\mathbf{F}'(-h_l)\mathbf{D}'(\mu_{l+1},\mu_l)] & (j\neq n) \\ \mathbf{I}' & (j=n), \end{cases} \end{cases} \tag{A8}$$

$$\bar{\mathbf{V}}_m = \begin{pmatrix} -(\bar{P}_{42}-\bar{P}_{44})\bar{\mathbf{Q}}_3^m+(\bar{P}_{32}-\bar{P}_{34})\bar{\mathbf{Q}}_4^m \\ (\bar{P}_{41}-\bar{P}_{43})\bar{\mathbf{Q}}_3^m-(\bar{P}_{31}-\bar{P}_{33})\bar{\mathbf{Q}}_4^m \\ (\bar{P}_{42}-\bar{P}_{44})\bar{\mathbf{Q}}_3^m-(\bar{P}_{32}-\bar{P}_{34})\bar{\mathbf{Q}}_4^m \\ -(\bar{P}_{41}-\bar{P}_{43})\bar{\mathbf{Q}}_3^m+(\bar{P}_{31}-\bar{P}_{33})\bar{\mathbf{Q}}_4^m \end{pmatrix}, \quad \bar{\mathbf{V}}'_m = \begin{pmatrix} -\bar{\mathbf{Q}}_2'^m \\ \bar{\mathbf{Q}}_2'^m \end{pmatrix}, \tag{A9}$$

$$\bar{\delta} = (\bar{P}_{31}-\bar{P}_{33})(\bar{P}_{42}-\bar{P}_{44})-(\bar{P}_{32}-\bar{P}_{34})(\bar{P}_{41}-\bar{P}_{43}), \quad \bar{\delta}' = \bar{P}'_{21}-\bar{P}'_{22}, \tag{A10}$$

with

$$\bar{\mathbf{P}} = \mathbf{G}^{-1}(\mu_1)\prod_{j=1}^{n-1}[\mathbf{F}(-h_j;\gamma_j)\mathbf{D}(\mu_{j+1},\mu_j)]\mathbf{E}(0;\gamma_n), \quad \bar{\mathbf{P}}' = \prod_{j=1}^{n-1}[\mathbf{F}'(-h_j)\mathbf{D}'(\mu_{j+1},\mu_j)], \tag{A11}$$

$$\begin{cases} \bar{\mathbf{Q}}^m = \begin{cases} \mathbf{G}^{-1}(\mu_1)\Pi_{j=1}^{m-1}[\mathbf{F}(-h_j;\gamma_j)\mathbf{D}(\mu_{j+1},\mu_j)]\mathbf{F}(H_{m-1}-d;\gamma_m)\boldsymbol{\Delta}(\gamma_m) & (m\neq n) \\ \mathbf{G}^{-1}(\mu_1)\Pi_{j=1}^{n-1}[\mathbf{F}(-h_j;\gamma_j)\mathbf{D}(\mu_{j+1},\mu_j)]\mathbf{Y}^s(H_{n-1};\gamma_n) & (m=n) \end{cases} \\ \bar{\mathbf{Q}}'^m = \begin{cases} \Pi_{j=1}^{m-1}[\mathbf{F}'(-h_j)\mathbf{D}'(\mu_{j+1},\mu_j)]\mathbf{F}'(H_{m-1}-d)\boldsymbol{\Delta}' & (m\neq n) \\ \Pi_{j=1}^{n-1}[\mathbf{F}'_j(-h_j)\mathbf{D}'(\mu_{j+1},\mu_j)]\mathbf{Y}'^s(H_{n-1}) & (m=n). \end{cases} \end{cases} \tag{A12}$$

Here, P_{ij}, P'_{ij}, $\bar{P}_{ij}$ and $\bar{P}'_{ij}$ are the ij elements of the matrices $\mathbf{P}$, $\mathbf{P}'$, $\bar{\mathbf{P}}$ and $\bar{\mathbf{P}}'$, and $\mathbf{Q}^m_k$, $\mathbf{Q}'^m_k$, $\bar{\mathbf{Q}}^m_k$ and $\bar{\mathbf{Q}}'^m_k$ are the k-th rows of the matrices $\mathbf{Q}^m$, $\mathbf{Q}'^m$, $\bar{\mathbf{Q}}^m$ and $\bar{\mathbf{Q}}'^m$, respectively.

Explicit expressions for $\mathbf{Y}^{(\prime)s}$ are given by

$$\begin{cases} \mathbf{Y}^s(z;\gamma_n) = \begin{pmatrix} 2 & -\mathrm{sgn}(z_d) & 2 \\ 4\mathrm{sgn}(z_d) & -1 & 0 \\ \mathrm{sgn}(z_d) & 0 & -\mathrm{sgn}(z_d) \\ -1 & 0 & 1 \end{pmatrix} + \gamma_n \begin{pmatrix} 1-3|z_d|\xi & z_d\xi & -1-|z_d|\xi \\ -4\mathrm{sgn}(z_d)+3z_d\xi & 1-|z_d|\xi & z_d\xi \\ -4\mathrm{sgn}(z_d)+3z_d\xi & 1-|z_d|\xi & z_d\xi \\ 1-3|z_d|\xi & z_d\xi & -1-|z_d|\xi \end{pmatrix}, \\ \mathbf{Y}'^s(z) = \begin{pmatrix} \mathrm{sgn}(z_d) & -1 \\ -1 & \mathrm{sgn}(z_d) \end{pmatrix} \end{cases} \tag{A13}$$

with

$$z_d = z - d, \tag{A14}$$

and the other matrices are defined as follows:

$$\boldsymbol{\Delta}(\gamma_m) = 2\begin{pmatrix} 0 & 1 & 0 \\ -4+4\gamma_m & 0 & 0 \\ -1+4\gamma_m & 0 & 1 \\ 0 & 0 & 0 \end{pmatrix}, \quad \boldsymbol{\Delta}' = -2\begin{pmatrix} 1 & 0 \\ 0 & 1 \end{pmatrix}, \tag{A15}$$

$$\begin{cases} \mathbf{F}(z;\gamma_l) = \begin{pmatrix} C(z) & -S(z) & 2S(z) & 0 \\ -S(z) & C(z) & 0 & 2S(z) \\ 0 & 0 & C(z) & S(z) \\ 0 & 0 & S(z) & C(z) \end{pmatrix} + \gamma_l \begin{pmatrix} z\xi S(z) & S(z)-z\xi C(z) & -S(z)+z\xi C(z) & -z\xi S(z) \\ S(z)+z\xi C(z) & -z\xi S(z) & z\xi S(z) & -S(z)-z\xi C(z) \\ S(z)+z\xi C(z) & -z\xi S(z) & z\xi S(z) & -S(z)-z\xi C(z) \\ z\xi S(z) & S(z)-z\xi C(z) & -S(z)+z\xi C(z) & -z\xi S(z) \end{pmatrix}, \\ \mathbf{F}'(z) = \begin{pmatrix} C(z) & S(z) \\ S(z) & C(z) \end{pmatrix} \end{cases} \tag{A16}$$

$$\mathbf{E}(z;\gamma_n) = \begin{pmatrix} 1 & 0 & 0 & \gamma_n z\xi \\ 0 & 2+\gamma_n(z\xi-1) & 1 & 0 \\ 0 & 1+\gamma_n(z\xi-1) & 1 & 0 \\ 1 & 0 & 0 & 1+\gamma_n z\xi \end{pmatrix}, \quad \mathbf{E}^{-1}(0;\gamma_n) = \begin{pmatrix} 1 & 0 & 0 & 0 \\ 0 & 1 & -1 & 0 \\ 0 & -1+\gamma_n & 2-\gamma_n & 0 \\ -1 & 0 & 0 & 1 \end{pmatrix}, \tag{A17}$$

$$\mathbf{D}(\mu_l,\mu_{l+1}) = \begin{pmatrix} 1 & 0 & 0 & 0 \\ 0 & 1 & 0 & 0 \\ 0 & 0 & \mu_l/\mu_{l+1} & 0 \\ 0 & 0 & 0 & \mu_l/\mu_{l+1} \end{pmatrix}, \quad \mathbf{D}'(\mu_l,\mu_{l+1}) = \begin{pmatrix} 1 & 0 \\ 0 & \mu_l/\mu_{l+1} \end{pmatrix}, \tag{A18}$$

$$\mathbf{G}(\mu_1)=\begin{pmatrix}1 & 0 & 0 & 0\\ 0 & 1 & 0 & 0\\ 0 & 0 & 1 & 0\\ 0 & \frac{\rho_1 g}{2\mu_1\xi} & 0 & 1\end{pmatrix},\quad \mathbf{G}^{-1}(\mu_1)=\begin{pmatrix}1 & 0 & 0 & 0\\ 0 & 1 & 0 & 0\\ 0 & 0 & 1 & 0\\ 0 & -\frac{\rho_1 g}{2\mu_1\xi} & 0 & 1\end{pmatrix}, \tag{A19}$$

with

$$\begin{cases} C(z)=\frac{1+\mathrm{e}^{-2z\xi}}{2},\quad S(z)=\frac{1-\mathrm{e}^{-2z\xi}}{2} & (z>0)\\ C(z)=\frac{\mathrm{e}^{2z\xi}+1}{2},\quad S(z)=\frac{\mathrm{e}^{2z\xi}-1}{2} & (z<0)\end{cases} \tag{A20}$$

Here, sgn(z) denotes the sign function, which takes the value of 1 for $z > 0$ and -1 for $z < 0$, ρ_1 the density of the surface layer, and g the acceleration due to gravity at the Earth's surface.